

Multifrequency Two-Dimensional Fourier Transform ESR: An X/Ku-Band Spectrometer

Petr P. Borbat, Richard H. Crepeau, and Jack H. Freed

Baker Laboratory of Chemistry, Cornell University, Ithaca, New York 14853

Received March 18, 1997

A two-dimensional Fourier Transform ESR (2D FT ESR) spectrometer operating at 9.25 and 17.35 GHz is described. The Ku-band bridge uses an efficient heterodyne technique wherein 9.25 GHz is the intermediate frequency. At Ku-band the sensitivity is increased by almost an order of magnitude. One may routinely collect a full 2D ELDOR spectrum in less than 20 min for a sample containing 0.5–5 nmol of nitroxide spin-probe in the slow-motional regime. Broad spectral coverage at Ku-band is obtained by use of a bridged loop-gap resonator (BLGR) and of a dielectric ring resonator (DR). It is shown that an even more uniform spectral excitation is obtained by using shorter microwave pulses of about 3 ns duration. The dead-time at Ku-band is just 30–40 ns, yielding an improved SNR in 2D ELDOR spectra of nitroxide spin-probes with T_2 as short as 20–30 ns. A comparison of 2D ELDOR spectra obtained at 9.25 and 17.35 GHz for spin-labeled phospholipid probes (16PC) in 1,2-dimyristoyl-*sn*-glycero-3-phosphoglycerol (DMPG) membrane vesicles showed that both spectra could be satisfactorily simulated using the same set of model parameters even though they are markedly different in appearance. The improved sensitivity and shorter dead-time at Ku-band made it possible to obtain orientation-dependent 2D ELDOR spectra of the Cholestane (CSL) spin-probe in macroscopically aligned lipid bilayers of egg yolk PC using samples containing only 1 mg of lipid and just 5 nmol of spin-probe. © 1997 Academic Press

Key Words: ESR; Fourier spectroscopy; Ku band ESR; multifrequency; heterodyne; sensitivity; lipids.

INTRODUCTION

Continuing progress during the last several years in the instrumental and theoretical development of two-dimensional Fourier transform ESR (2D FT ESR) spectroscopy (1, 2) has resulted in a variety of successful applications to a wide range of systems including simple and complex fluids, membranes, polymers, and solids. In particular, the increased sensitivity of 2D FT ESR correlation spectroscopy to molecular ordering and dynamics has made it possible to extend our knowledge about the dynamic molecular properties of liquid crystals (3, 4), polymers (5), and membrane vesicle dispersions (6), including peptide–lipid interactions (7).

Thus, this powerful method offers the opportunity to study complex materials and biologically relevant systems. Unfortunately, biological samples are typically available in small quantities, requiring very high sensitivity, which until recently could only be obtained with continuous wave (CW) ESR spectroscopy. Also, in the initial applications of 2D FT spectroscopy to model membrane vesicles using standard spin-probes, some discrepancies were found between the 2D FT ESR results and the CW ESR results (6). As in CW ESR, an improved understanding of 2D ELDOR should be achieved by comparative experiments on macroscopically aligned lipid membranes. Such experiments have not yet been performed due to the need to use very small volumes of oriented membranes because of the constraints of the small bridged-loop-gap resonator used in 2D FT ESR, and this again leads to a serious problem with sensitivity. Thus, the problem with sensitivity is a general one.

Another problem is the relatively low mobility of the spin-probes that are commonly used in membrane studies, which leads to slow-motional broadening. This, in turn leads to a large inhomogeneous broadening $1/T_2^*$ which results in a very rapid free induction decay (FID), as well as a short homogeneous T_2 which results in the loss of a substantial portion of the signal due to the spectrometer dead-time, hence poorer sensitivity.

A partial solution to these problems may be achieved by performing 2D FT experiments at higher frequencies where one can expect increased sensitivity and shorter dead-times. Furthermore, frequency constitutes an important variable in ESR spectroscopy as a result of its effect on the spin Hamiltonian, which is modulated by the molecular motions. An increase in magnetic field and frequency allows one to shift the more informative slow-motional regime to the region of shorter correlation times, as has been shown in CW ESR work at millimeter waves (8). Moreover, performing 2D FT ESR experiments over a broad range of frequencies would provide greater insight into the subtle details of motional dynamics that could not be reliably extracted in an experiment at a single frequency.

Until recently 2D FT ESR correlation spectroscopy has

been performed only at X band (9). Here we report on the development and use of a spectrometer that operates at 17 GHz as well. In the next sections we briefly address the technical problems associated with multifrequency 2D FT spectroscopy. We then describe our X/Ku band 2D FT microwave bridge and provide the results of comprehensive tests where we emphasize applicability to model lipid membrane systems in the form of vesicle dispersions and of macroscopically aligned lipid multilayers.

THEORETICAL AND PRACTICAL CONSIDERATIONS

General

FT NMR was initially introduced as an improvement on the signal-to-noise over CW detection, due to its multiplex approach (10). FT ESR, on the other hand, was developed primarily to improve the study of dynamic processes such as molecular motions (1, 3–9) and the spin chemistry of short-lived reaction intermediates, which take place on the submicrosecond time-scale (11–13). While 1D FT ESR has been applied successfully to the latter, the former has motivated the development of 2D ESR methods. Early forms of 2D ESR utilized 2 and 3 pulse spin-echo sequences with selective excitation for mapping out the variation of the homogeneous linewidth across the ESR spectrum and the variation of the magnetization transfer across the ESR spectrum, respectively (14, 15). With significant instrumental developments, Gorcester and Freed (1, 9, 16) and Bowman (2, 11) were able to conduct 2D FT ESR experiments on motionally narrowed spectra from organic radicals. A major hurdle remained, which was to study by 2D FT ESR the typical slow-motional spectra arising from nitroxide spin-labels with their very broad shapes and rapid relaxation times. The key instrumental and theoretical challenges to operation at X-band have been largely overcome in recent years (17, 18). These instrumental challenges are, in general, much greater than in NMR due to the use of microwave vs RF technology, nanosecond vs millisecond relaxation times, and spectral bandwidths greater than 100 MHz vs kHz bandwidths. These 2D FT ESR experiments on motional dynamics are to be contrasted with the most widespread application of pulsed ESR, which has been to structural studies on solids, where relaxation times are much longer, one does not capture the full echo shape or the free induction decay, and bandwidths required are relatively small (19–21). In fact, whereas pulsed ESR spectrometers for a wide range of frequencies have been developed, they have all been developed for application to structural studies in solids. In general, spectrometers operating below 35 GHz are homodyne; while those operating at higher frequencies are usually heterodyne (22, 23).

The recent development of 2D FT correlation spectroscopy is largely due to major technical advances in the fields

of high-speed electronics and microwave technique. Progress in fast digitization and signal processing techniques allows one to capture signals with nanosecond time resolution and with a bandwidth of several hundred megahertz, and to average these signals at rates of 10 kHz (6) and even faster (cf. below). There are still a number of significant compromises required, given the performance characteristics of existing microwave and digital components that are needed for FT ESR instrumentation. But we believe the remaining challenges are likely to be satisfactorily addressed in the near future.

Frequencies in the X to Ka bands (i.e., 8–35 GHz) are suitable for 2D FT-ESR spectroscopy due to the availability of convenient pulsed high-power microwave sources such as traveling wave tube amplifiers (TWTA). Broadband frequency tuning is not necessary, thereby simplifying technical implementation. Our FT ESR spectrometer described herein operates in both the X and Ku microwave bands. We employ a heterodyne technique to conveniently and reliably implement 2D FT ESR at Ku band (17.3 GHz). A low-power microwave section of a pulsed ESR spectrometer with working frequency to Ka band can be designed, in principle, using proven homodyne techniques. For a multifrequency FT ESR spectrometer, a significant reduction in microwave components and improved performance may be achieved by using, at the different frequency bands, the same 'building blocks' for the low-power sections of the expensive transmitter and receiver parts of the spectrometer, if it is to be based on heterodyne methods.

The three major technical features that determine the performance of an FT ESR spectrometer are (1) spectral excitation bandwidth, (2) sensitivity, and (3) spectrometer dead-time. We discuss them briefly below.

Spectral Excitation

For purposes of 2D FT ESR correlation spectroscopy such as COSY or 2D ELDOR, it is necessary to excite the whole ESR spectrum. ESR spectra can have an extent of several hundred gauss corresponding to GHz bandwidths. It would be very difficult to achieve excitation over such a broad frequency region. Here we are concerned with full spectral excitation for nitroxide spin-probes. In the slow-motional regime, this corresponds to a spectral extent of about 70 G, or 200 MHz for both X and Ku bands. This gives us a lower limit on the acceptable spectral excitation bandwidth. An excitation bandwidth of 2Δ , when only limited power is available from an excitation source, imposes a severe limit on the effective resonator volume, V_c . That is, from steady-state arguments (1, 9),

$$P_0 = V_c(2B_1)^2\omega/2\mu_0Q_L \quad [1]$$

which relates the circular component of the microwave

(mw) field B_1 at the sample to the mw power P_0 dissipated by the resonator. In Eq. [1], ω is the resonant frequency and Q_L is the resonator's loaded quality factor. P_0 is equal to the mw power incident on the resonator if the resonator is matched. The half-power full bandwidth of the resonator is given by ν/Q_L ($\nu = \omega/2\pi$), which we set equal to 2Δ to ensure it can accommodate this excitation bandwidth. Also, the half amplitude excitation bandwidth $\Delta\nu$ provided by the mw radiation is approximately $5.4 \gamma_e B_1/2\pi$ for one $\pi/2$ pulse (24), which we also set equal to 2Δ . Substituting into Eq. [1] we find that $P_0 \propto \Delta^3 V_c$. Thus the volume of the resonator that is needed obeys

$$V_c \propto P_0 \Delta^{-3}. \quad [2]$$

The maximum power available is limited for two major reasons. First is the availability and the price of the source, and second is the serious problems associated with protecting the receiver and with its recovery after an overload from pulses that are about a kilowatt at the source. Due to the cubic dependence of the required power on Δ , the ability to excite very wide spectra is limited, unless one reduces the size of the resonator (I), which ultimately reduces the size of the sample one can use.

Sensitivity

The signal-to-noise ratio (SNR) per unit time (more precisely: per $t^{1/2}$) in 1D or 2D spectra may be found from the expression for the SNR of the time domain signal at the output of the matched resonator produced by the precession of the macroscopic magnetization, $M = M_0 s(t_1, t_2)$. Here $s(t_1, t_2)$ is the envelope function of M . In the 1D case it is a function of t_2 only. According to general analyses of sensitivity for ESE (19, 25), we may write

$$\text{SNR} = M_0 E f_c^{-1/2} \{s(t_1, t_2) * K(t_2)\}, \quad [3]$$

(where the asterisk implies a convolution). Here $M_0 = Ng^2\beta^2 S(S+1)B_0/3kT$ is the static magnetization of the sample with N the number of spins in the sample; $E = \sqrt{\mu_0\omega Q_L/8V_c kTF_N}$ is the sensitivity factor; k is Boltzmann's constant; $B_0 = \omega/\gamma$ is the static magnetic field; f_c is the noise frequency bandwidth; F_N is the receiver noise figure; and $K(t_2) = (2\tau_r)^{-1} \exp(-t_2/2\tau_r)$ is the time response function of the resonator itself, with $\tau_r = Q_L/\omega$ being the resonator time constant. More rigorously, $K(t_2)$ should be the time response function of the whole receiver system, but that of the resonator is the principal contributor. It should be noted that, since the expression for E was obtained from considerations of equivalent RF circuits or from CW sensitivity, this expression should be regarded as an approximate estimate rather than an accurate result.

Following the discussion in Refs. (9, 10) and including

Eq. [3], we obtain for the 1D case, when an FID is detected, the expression for the SNR per unit time, (i.e. per $t^{1/2}$):

$$\text{SNR} = \frac{2}{5} M_0 E K(\omega_2) \left(\frac{2t_{2\max} f_{\text{rep}}}{N_{\text{int}}} \right)^{1/2} \times \exp\left(-2t_d \left(\frac{1}{T_2^*} + \frac{1}{T_2} \right)\right), \quad [4]$$

where $K(\omega_2) = (1 + (2\omega_2\tau_r)^2)^{-1}$ is the resonator response (or else the general system frequency response); $t_{2\max}$ is set equal to $5T_2^* T_2 / (T_2^* + T_2)$, so that the signal should decay to 1% of its initial value. Also, N_{int} is the number of interleaves, and we set the input frequency bandwidth to the Nyquist frequency $f_c = m_2 N_{\text{int}} / (2t_{2\max})$, where m_2 is the number of samples in a single pulse sequence, f_{rep} is the repetition frequency of the pulse sequences, and t_d is the dead-time. For the 2D case we may consider either 2D ELDOR or COSY with the echo-like S_{C-} signal component (referred to as the N component in NMR (10)). We take the envelope function of the S_{C-} signal to be of the form $s(t_1, t_2) = \exp(-t_1/T_2) \exp(-t_2/T_2) \exp(-|t_1 - t_2|/T_2^*)$. By analogy to the derivation of Eq. [4], we take $2t_{1\max}$ and $2t_{2\max}$ equal to $5T_2$. Assuming $T_2^* \ll T_2$, we obtain

$$\text{SNR} = \frac{4}{25} M_0 E K(\omega_2) \left(\frac{2t_{2\max} f_{\text{rep}}}{N_{\text{int}}} \right)^{1/2} \times \left(\frac{T_2^*}{T_2} \right) \exp\left(-\frac{2t_d}{T_2}\right). \quad [5]$$

For a typical case $t_{2\max} = 100$ ns, $T_2 = 4T_2^*$, $f_{\text{rep}} = 10$ kHz, $N_{\text{int}} = 5$, $F_N = 6$ dB, $V_c = 50 \times 10^{-9}$ m³ we find that at 17 GHz the minimal detectable number of spins is $N_{\text{min}} = 2 \times 10^{13}$ spins/ $s^{1/2}$.

In the following analysis we evaluate the frequency dependence of the sensitivity of FT spectroscopy. Thus we are primarily interested in the frequency dependence of the product EM_0 in Eqs. [4] and [5]. It is proportional to $\omega^{3/2} N Q_L^{1/2} F_N^{-1/2} V_c^{-1/2}$, and to a large extent is related to the excitation bandwidth. We also assume the B_1 and excitation bandwidth to be constant. Then

$$\text{SNR} \propto \frac{\omega^{3/2} N Q_L^{1/2}}{F_N^{1/2} V_c^{1/2}}. \quad [6]$$

The receiver noise figure F_N does not depend greatly on frequency over the X and K bands, but varies no more than 4–6 dB. Because $Q_L \propto \omega/\Delta$, for the case of full spectral excitation we may write

$$\text{SNR} \propto \omega^2 N V_C^{-1/2}. \quad [7]$$

Thus,

$$N_{\min} \propto \omega^{-2} V_C^{1/2} = \omega^{-2} V_S^{1/2} \eta^{-1/2} \quad [8]$$

or alternatively

$$(N/V_S)_{\min} \propto \omega^{-2} \eta^{-1} V_C^{-1/2}. \quad [9]$$

Here, N_{\min} is the minimum number of detectable spins, and $(N/V_S)_{\min}$ is the minimum detectable concentration. Also V_S is the volume of the sample, which is related to V_C as $V_S = \eta V_C$, with η the filling factor. If we use the same type of resonator for the different frequencies, but construct them such that their linear dimensions are inversely proportional to ω , and we have the same filling factor η , then N_{\min} is proportional to $\omega^{-7/2}$. However, this does not lead to an appreciable improvement in concentration sensitivity. The $(N/V_S)_{\min}$ will vary with frequency only as $\omega^{-1/2}$, and this gain will be reduced by a small degradation of the noise figure at higher frequencies.

If we again scale the dimensions in the same fashion, but keep the incident power and Q_L constant, then $N_{\min} \propto \omega^{-3}$ and $(N/V_S)_{\min}$ does not change. The excitation bandwidth will increase as ω , while a $\pi/2$ pulse of duration $t_{\pi/2}$ will decrease as $1/\omega$ to match the excitation bandwidth. Thus we improve both the excitation bandwidth as ω and the detection limit as ω^{-3} .

For samples that are not limited in volume, one can choose a volume appropriate for the size of the resonator, which, in turn, depends on the excitation bandwidth through Eq. [2]. Provided there is sufficient power at each frequency to keep both V_C and η the same at the various frequencies, then both N_{\min} and $(N/V_S)_{\min}$ will be proportional to ω^{-2} and the excitation bandwidth is the same.

Thus, we see that at higher frequencies it is possible to get considerable improvement in sensitivity and/or in spectral coverage. For improved spectral coverage, one may, for example, use a smaller resonator with the same Q_L at the higher frequency, which would increase the bandwidth, (i.e. $2\Delta = \nu/Q_L$). Commercially available pulsed broadband TWTAs are capable of delivering about the same 1–2 kW of peak power at both X and Ku bands. Assuming that the required excitation bandwidth is 200 MHz, and $P \sim 1$ kW, we find from Eq. [1] that $V_c \sim 150 \mu\text{L}$. Such requirements on the effective volume can be satisfied at X band only with lumped structures such as loop-gap resonators, dielectric resonators, or slow-wave structures. Actually, at X band we use bridged loop-gap resonators (BLGRs) with an effective volume of about 80–100 μL . Fortunately, lumped resonators with the needed effective volume can be constructed for Ku band,

giving us the opportunity to increase the concentration sensitivity in going to Ku band.

The Dead-Time in FT Spectroscopy

Dead-time is a crucial feature of a FT ESR spectrometer. It has been discussed in connection with the design of various ESE spectrometers that have been constructed at different frequencies (2, 23, 25–27), and Gorcester *et al.* (1, 9) have discussed it in the context of 2D FT ESR. The dead-time has been defined in different ways in the literature depending on the particular application. We define it here as the time interval from the end of the last excitation pulse (i.e., the readout pulse) to the point where an exponentially decaying FID signal is within 10% of the magnitude that would be measured at that point for the case of zero dead-time, and it is distorted by less than 10% at longer times. We often find that the signal, which should be a decaying function, starts to grow from the baseline during a 5–10 ns period before it reaches 0.9 of its expected value. This growth occurs during the period of receiver recovery from saturation after the pulse. If it is possible to recover the signal during that time, then the dead-time will be 5–10 ns shorter. At present we have not developed a reliable procedure to utilize this initial distorted signal. One possibility would be to observe the FID of a signal with one or more very sharp lines (e.g., PD-Tempone in toluene, cf. Ref. (9)) for which linear predictive methods can reliably be used to back-extrapolate the FID to zero dead-time. A comparison of the observed results during the receiver recovery period with the back-extrapolation should yield an instrumental correction function for reconstructing the initial part of the signal.

For a 2D ELDOR experiment, where all background signals are canceled by choosing a proper phase cycle sequence (28), the dead-time is shorter than for a one-pulse FID or a two-pulse COSY sequence. For an FID from a single pulse it is not possible to subtract all the background signals by phase cycling, so the resulting dead-time is 20–40 ns longer than for 2D ELDOR in our spectrometer, depending on frequency, shielding, etc. With an additional subtraction (“signal” – “no signal”) we found the dead-time to be the same as for 2D-ELDOR for any pulse sequence, with a maximum $\sqrt{2}$ penalty in SNR. For time-resolved FID ESR spectroscopy utilizing a single pulse, subtraction of this type can be performed so our dead times will be referred to this case. For purposes of FID ESR on transient radicals, it would be desirable to detect a signal as early as possible after the pulse, even if it is not possible to recover it completely. With our spectrometer, we can, for example, detect an FID signal 30–35 ns (or even less) after the *beginning* of the (2–5 ns) excitation pulse.

There are several major factors that determine the dead-time of an ESE spectrometer. When dead-times in excess of 80–100 ns are acceptable, as is usually the case for ESEEM

spectroscopy, their major source in a well-designed system is the ringing down of the resonator. For dead-times of 50 ns or less, this is not necessarily the case. The problem has been considered in connection with ESE spectrometers working at much higher frequencies, where a resonator time constant $\tau_r = Q_L/\omega$ can easily be made very short (27). In that case, reflections of the exciting microwave pulse in the waveguide were found to constitute an important mechanism for increased dead-time. That reason tends to be important in the millimeter wave range, because reflections at high frequencies are typically larger. It was also found (27) that the sharp edges of the excitation pulse exhibit noise-like behavior due to their broad Fourier spectrum, their instability, and the multiple reflections. The background signal resulting from this feature of the pulses is difficult, if not impossible, to digitize with existing digitizers in order to subtract it from the signal of interest, even if it does not overload the receiver.

Let us first consider the effects of resonator ringing. One typically finds that a 1-kW pulse must decay about 140 dB to reduce the power level to that of the input noise ($I, 9$). The level to which power at the receiver input must decay depends on the dynamic range of the receiver. For a dynamic range of 60 dB, the power should decay from its 60 dBm maximum to approximately -20 dBm, i.e., by a $\Delta P = 80$ dB. Given a resonator with $Q \approx 240$, the time constant, τ_r at 9.4 GHz is about 4 ns. Then the corresponding damping, d_r defined as

$$d_r \equiv -10 \log[\exp(-10^9/\tau_r)] = 10^8/2.3\tau_r, \quad [10]$$

is ~ 1.1 dB/ns, and it results in a dead-time $\tau_d \sim \Delta P/d_r$, i.e., 74 ns. To obtain a shorter dead-time, τ_r should be reduced. For $Q_L \sim 50$ at 9.4 GHz, τ_r is 0.85 ns (so d_r is 5.1 dB/ns). On the other hand, for such a short τ_r , it is desirable to have an analog bandwidth of the digitizer of $\sim 1/4\tau_r$ to be able to capture and to subtract out the rapidly decaying tail of the overloading pulse. For $\tau_r \sim 0.85$ ns the bandwidth should be of order 300 MHz. Digitizers working with adequate analog bandwidth for full-scale signal have only a 40 dB dynamic range; hence ΔP is increased by 20 dB, resulting in a τ_d of 20 ns for the case where reflections can be neglected.

The role of reflections in the waveguide system can be estimated in a simplified way. Let us consider a waveguide of length L with reflection coefficients Γ_1 and Γ_2 at the ends. If a pulse propagates in the direction from end 1 to end 2 with group velocity v_g , then the fraction of the power $|\Gamma_2| \times |\Gamma_1|$ reflected back from end 2 and then from end 1 arrives at end 2 delayed by $2L/v_g$. It continues to reflect back and forth between ends 1 and 2, leading to a finite decay. It is convenient to express the effects of the reflections as return loss, measured in decibels, $R = 20 \log |\Gamma|$, and

to introduce an effective damping in the waveguide d_w by analogy to d_r . For an estimate of d_w , we simply divide the return loss accumulated in multiple reflections by the propagation time (cf. Eq. [10]). This gives an estimate:

$$d_w \approx -\frac{v_g 10 \log(|\Gamma_1| |\Gamma_2|)}{L} \times 10^{-9} (\text{dB/ns}). \quad [11]$$

To reduce dead-time caused by reflections in the waveguide, it is necessary to increase d_w . For a well-matched waveguide section of length 0.8 m with VSWR at both ends of about 1.1 (26 dB return loss), reflected power decays with an effective damping $d_w \sim 8.1$ dB/ns, which is generally adequate. To construct a waveguide system that is perfectly matched over a broad frequency range may be extremely difficult, if not impossible. If the waveguide is not well-matched at one end (for example, a strongly overcoupled resonator is there), d_w decreases by about a factor of 2, and the observed dead-time $t_d \approx \Delta P/(d_w^{-1} + d_r^{-1})$ would be considerably longer than is imposed by the ring down of a low-Q resonator itself.

Another source of dead-time is the high-power pulsed TWTA, since it does not turn off instantly. Typical values for the turn-off time of a pulsed TWTA are 10–50 ns. For the Logimetrics' EPA740I/J TWTA that we are currently using, it is close to 20 ns, largely due to the turn-off performance of the grid modulator. There is noise output that lasts at least during that time period, when it falls rapidly. It has a broad frequency spectrum, and it tends to decay slowly at a later time, in part, due to reflections. By reason of the high gain and noise figure of the TWT amplifier, that noise is well above receiver saturation and results in a dead-time contribution of 25–40 ns. An improved modulator design providing rapid turn-off for a Litton 620 TWTA of approximately 10 ns is described in Ref. (1).

Another significant source of dead-time is the recovery of the saturated components in a receiver. Our fast diode limiter recovers to 1 dB of its normal insertion loss in 10–20 ns after overloading by a 100 W pulse, resulting in a dead-time of about 15–25 ns. For microwave amplifiers, manufacturers usually specify similar recovery times after hard saturation. We measured shorter values of 5–10 ns.

Considering all of the above factors, we arrive at the conclusion that it would not be possible to reach dead-times any more quickly than in about 25–30 ns with the design we employ. The shortest dead-time we have achieved was 30 ns when we utilized a TWTA with a rapid (10 ns) modulator turn-off time. Any significant improvements in dead-time would, in our estimation, require the use of a bimodal resonator with an isolation of at least 50–60 dB. The bimodal resonator would perform the useful function of protecting the receiver from all the above sources of dead-time, except for reflections in the bridge after the resonator. Even

with such a bimodal resonator, 10–15 ns would appear to be a practical limit on the dead-time. For lossy samples (e.g., aqueous samples) which strongly affect the resonator (29), it may be difficult to achieve such high mode isolation. Nevertheless, bimodal structures (30), even in the case of reduced isolation, should still be very useful in helping to bring the slowly decaying TWTA noise output down to a level where it could be averaged out.

THE SPECTROMETER DESIGN AND PERFORMANCE

In constructing our 2D FT spectrometer, particular emphasis was placed on its applicability for the study of the dynamics of nitroxide spin-probes in the slow-motional regime at two distinct frequencies differing by about a factor of 2. Tuning over a broad frequency range was not required; thus performance could be optimized over a limited tuning bandwidth, such as 0.5 GHz for each frequency. Such a bandwidth is sufficient to compensate for resonant frequency variations of the resonator caused by insertion of a sample or by a temperature change. In principle, it is possible to build a homodyne pulsed microwave bridge for each frequency (26, 31, 32). On the other hand, this is the more expensive approach, and devices capable of providing precise phase control that are required for the purposes of 2D FT ESR at higher frequencies are either not readily available or have poorer specifications and are more expensive. As is well known, heterodyne techniques can be used to solve these problems with phase control and cycling, and only a few components specific to the higher frequency are required.

A block-diagram of our X/Ku band 2D FT ESR spectrometer microwave bridge is shown in Fig. 1. For signal acquisition in the experiments reported below we used a pair of TRAQ-H 200 Msp/s transient digitizers from DSP Technologies, each capable of averaging 256 word records at a 10 kHz rate simultaneously on both channels. Very recently we have incorporated a system with faster data throughput. For spectrometer timing with high time resolution we use four digital delay generators (DG535A) from Stanford Research Systems.

The microwave bridge (cf. Fig. 1) operates as a homodyne FT ESR bridge at X band that resembles other ESE and FT-ESR spectrometers designed for X-band (1, 2, 20, 21, 31). Its X band option is a restructured and completely rebuilt version of our original 2D FT-ESR X-band bridge (16). It includes two microwave pulse forming channels. Each of them is able to form microwave pulses as narrow as 3–5 ns with four possible phases. The phases are produced with the help of 2-bit quadrature phase shifters (QM1, QM2) optimized at 9.25 ± 0.25 GHz to meet the requirements of 2D FT ESR spectroscopy. An additional 45° phase shifter, common to both branches, was added for double-quantum coherence experiments (33). At Ku band (17.35 GHz) it operates as a heterodyne bridge, with 9.25 GHz used as the

intermediate frequency. It is this frequency at which the 2-bit phase shifters and the quadrature mixer are the most accurate. Each of the two channels contains an electromechanical transfer switch (SW1, SW2) for band selection. For Ku band operation, by switching on (SW1, SW2), mixers are placed into the signal path to convert the phase-encoded X band CW output of the quadrature phase shifters to Ku band by mixing with a local oscillator, tunable around 8 GHz. For the local oscillator, we used a microwave synthesizer, Giga-Tronics 1018. It has just been replaced with a much less expensive module sufficient for tuning over 500 MHz bandwidth. Fast broadband PIN diode switches (PIN1, PIN2) are used to form microwave pulses that are later combined and amplified by a low-noise amplifier (LNA) A4. An extra broadband PIN diode switch (PIN3) with less than 1 ns fall time was placed at the TWTA input. It is used to obtain shorter microwave pulses and to increase the isolation of the TWTA input from the CW source.

Many modern ESE spectrometers have more than one pulse-forming channel to produce microwave pulses of different amplitudes or to facilitate phase cycling (1, 20, 21, 32, 34). The second pulse-forming channel is required to reduce the time separation between the second and third pulses in the 2D ELDOR pulse sequence. The recovery time of the 2-bit phase shifters that are currently employed limits interpulse separation by 25–30 ns within a single channel. With the second channel, the pulse separation can be reduced to 5 ns. Different amplitudes of pulses in a microwave sequence are not required in 2D ELDOR. Nevertheless, it is a useful feature for HYSORE (20), and it is necessary for Pulse Adjustable Spectroscopies (PAS), where arbitrary pulses are used (35, 36).

The receiver section was modified in a manner similar to the transmitter. The Ku band preamplifier, the frequency converter, and one more transfer switch (SW3) have been added. Of course, it is possible to use a single broadband LNA for both bands. Other details should be clear from Fig. 1. The intermediate frequency of 9.25 GHz, which was dictated by the performance of the existing microwave components, was not very convenient for obtaining a broad frequency tuning range at Ku band because its second harmonic was sufficiently close to the working frequency bandwidth. A tuning bandwidth of 17.35 ± 0.25 GHz was achieved. This is sufficient to compensate for small resonant frequency changes caused either by the sample or by temperature change.

Several different resonators were constructed and tested for Ku band. At X band we use a BLGR with a 3.4 mm i.d. and a length of 8 mm. It has an effective volume of about 80–100 μL . This resonator is coupled to the waveguide with a 3.5-mm diameter loop, and its Q_L may be adjusted from 50 to 100 to obtain the desired bandwidth. With thin-walled 2.5 o.d. sample tubes, we have a sample volume of up to 20 μL . At Ku band we initially used a small TE_{102} cavity

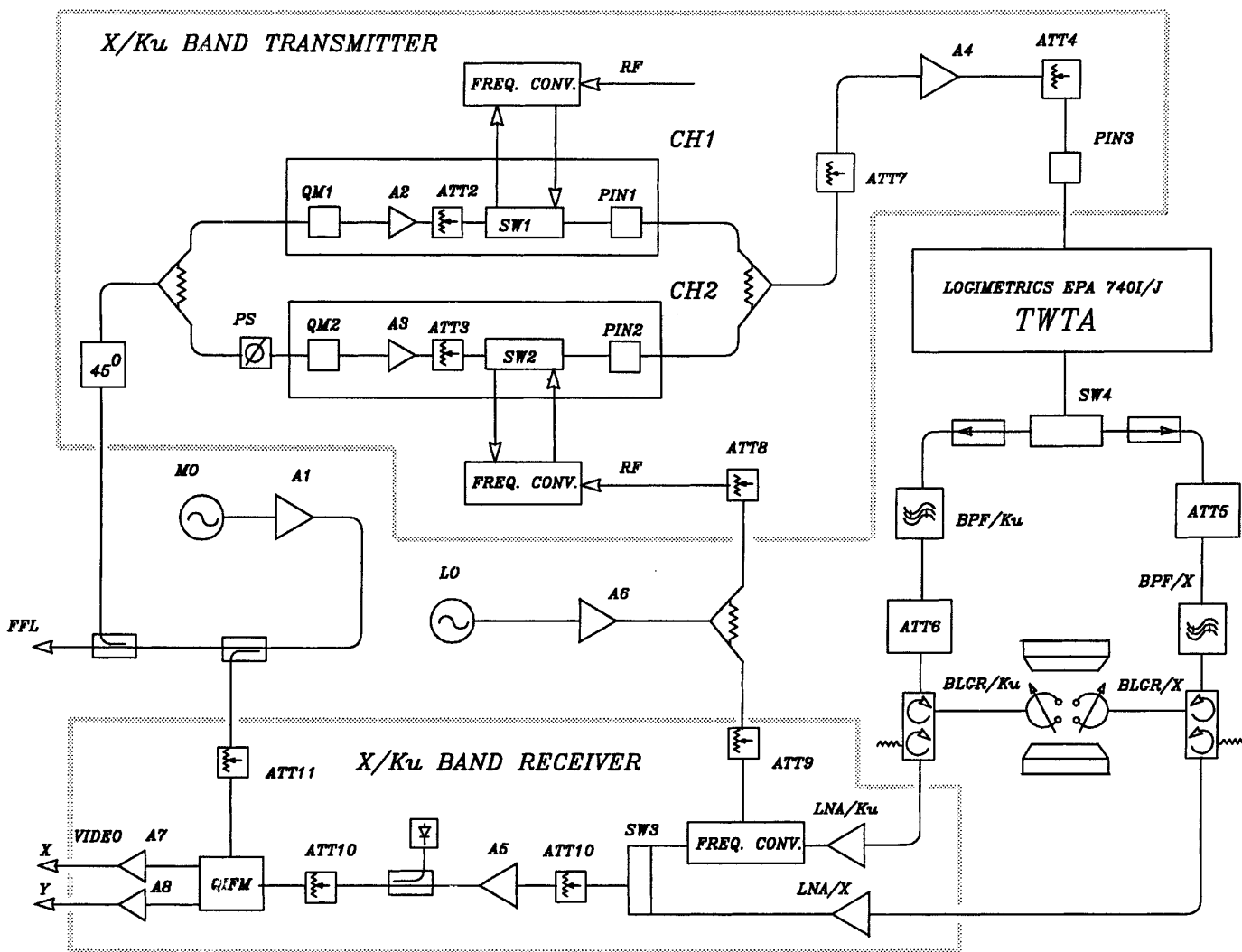


FIG. 1. Schematic diagram of the microwave part of the X/Ku band 2D FT ESR spectrometer. MO, HP8672A synthesized sweep generator (Hewlett-Packard); QM1, QM2, quadrature phase shifters, DP629.25HS (Vectronics Microwave); PS, phase shifter (ARRA); ATT2, ATT3, PIN diode attenuators, D1958 (General Microwave); A2, A3, X-band amplifier N6244S (NARDA Microwave); SW1, SW2, electromechanical DPDT switch; PIN1, PIN2, PIN diode switches, P/N 2662 (M/A-COM); FREQ. CONV., frequency mixer M50AC (Watkins-Johnson Co.) and bandpass filter; PIN3, PIN diode switch SWN-AGRA-GAK0-ECL-LVT, (American Microwave Corp.); A6, X band low-noise amplifier (Avantek); "45°", home built switched line 45° phase shifter; LO, synthesized sweep generator, Giga-Tronics 1018; A5, A6, X-band microwave amplifiers; ATT XX, various microwave attenuators; A1, A4, low-noise amplifiers APM180-2336 (CTT); LNA/Ku, low-noise amplifier DB95-0908 (DBS microwave, Inc.); LNA/X, low-noise amplifier AMF-23-8897-23-LM (MITEQ); SW3, electromechanical SPDT switch (RLC); QIFM, quadrature mixer IRD12F09FM (RHG); A7, A8, videoamplifier CLC100 (Comlinear); FFL, X-band FFL system, Varian V-4542; BPF X/Ku, waveguide bandpass filters. The purpose of other typical components, such as power dividers and combiners, detectors, and directional couplers, are clear from the diagram. The high-power lines were built using WR90 and WR62 waveguide, waveguide attenuators, and ferrite devices. DC-blocks and isolators were installed where they were necessary. LNA inputs were protected with a diode limiter ACLM-4906 (Advanced Control Components, Inc.).

resonator having an effective volume $V_e \sim 200 \mu\text{L}$ or about 2.0–2.5 times larger than that for the BLGR used at X band. With this resonator, after reduction of its Q_L by microwave absorbing material, it was possible to obtain $\pi/2$ pulses ranging from 8 to 13 ns depending on the Q_L , which ranged from 80 to 200. Tuning was either by a Gordon or by a screw coupler. The dead-time of 33–40 ns even at $Q_L \sim 150$ –200 was shorter by about 10 ns than we usually mea-

sured at X band. The sensitivity varied with Q_L , being only 1.5 times larger relative to X band, due to the low filling factor of the TE_{102} resonator. It was not possible to obtain the same spectral coverage as at X band due to the larger volume V_e and the 5–6 dB loss of power in the waveguide parts. This resonator is useful for its simplicity, and it is less sensitive to lossy samples. It is not really adequate for 2D ELDOR with slow-motional nitroxides due to the reduced

spectral coverage. For 1D FT spectroscopy it could be used without significant problems.

We then constructed a BLGR of about the same size as we currently use at X band. Unlike its X band predecessor, we coupled it to the waveguide using a Gordon or screw coupler. Due to sufficiently low unloaded $Q_u \sim 200$, it was possible to obtain critical coupling at the desired $Q_L \sim 100$ or to overcouple it to $Q_L \sim 50$. An exception was for the case of very lossy samples, where it was often only possible to undercouple. In addition to the BLGR, which is difficult to make, we used at Ku-band a sapphire dielectric ring resonator (DR) with dimensions $6.5 \times 2.8 \times 5$ mm that admits a sample of the same size as at X band, except for samples with higher loss. For the DR, it was necessary to spoil its unloaded, Q_u in order to avoid large overcoupling. It was sufficient to use small lossy pads of microwave absorbing material made of "antistatic" packaging envelopes to bring Q_u down to 200–400. Test samples used to compare the sensitivity at both frequencies were a small sample of lithium phthalocyanine, and a 20- μ L sample of 1 mM solution of perdeuterated TEMPONE (PDT) in toluene sealed off in 2.5-mm o.d. thin-walled glass tubes. The sensitivity was compared as the SNR of the FID signal as it appears on the scope screen. Experimenting with the same standard samples as at X-band, we found that the sensitivity at 17.3 GHz was usually 3–4 times better with a critically coupled BLGR, as we expected. However, up to eight times better sensitivity was obtained when the DR was used in an overcoupled fashion (2, 19, 37). There was a small reduction in the excitation bandwidth, due to greater loss of power in the waveguide parts. The dead-time was within 30–40 ns. We attributed the additional enhancement in SNR above that predicted theoretically (cf. Eq. [7]) to nonoptimal conditions at X band, where we avoided overcoupling because it increases dead-time, and to the concentration of the B_1 field into a somewhat smaller volume for the case of the DR.

In considering spectral coverage, we note that the requirement imposed by the excitation bandwidth is somewhat different for FID spectroscopy utilizing a single excitation pulse, and for 2D ELDOR spectroscopy requiring three pulses (1, 2, 9, 24). For the 1D case and a given B_1 , a more uniform excitation will be obtained with a shorter pulse, corresponding to less than a $\pi/2$ rotation. Figure 2 demonstrates, for PDT, the spectral excitation at 17.3-GHz by pulses with different widths ranging from 3 to 6 ns, and the coverage profile measured with the use of a single 3-ns pulse. It is clear from the figure that a 3-ns pulse rotates the spectrum by an angle of about $\pi/4$, which reduces the signal in the center by a factor of 0.7 while outermost line grows with shortening of the pulse. This effect is multiplicative for the three pulses of 2D ELDOR. Our objective was to obtain sufficiently broad coverage in the 2D ELDOR experiment for nitroxide spin-probes corresponding to a spectral extent of about 200 MHz. From this requirement it follows that the

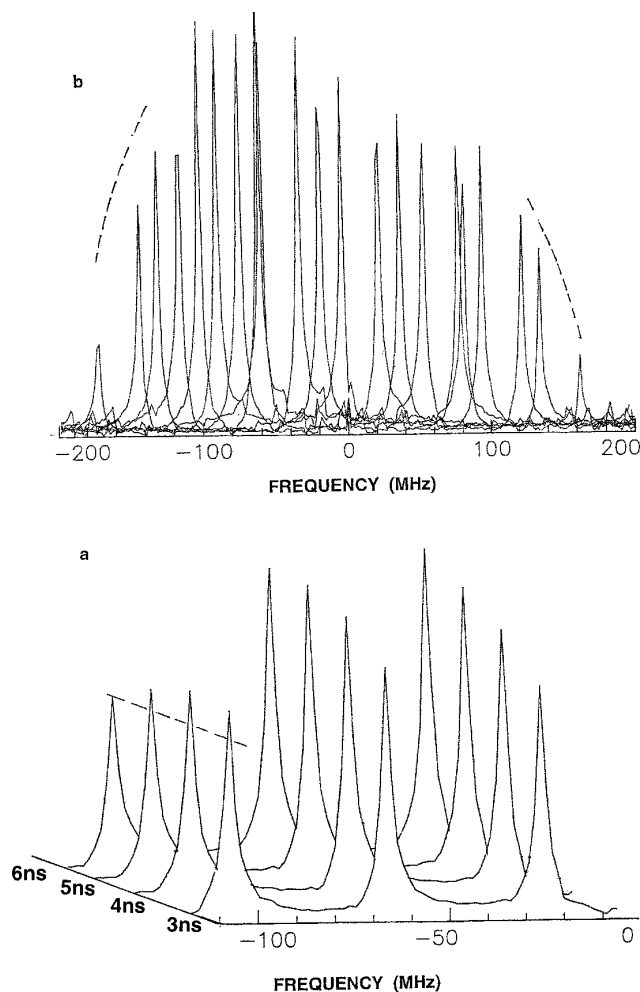


FIG. 2. Measurements of spectral coverage at 17.35 GHz using a bridged loop-gap resonator and a sample of 1 mM solution of PDT in toluene. (a) Stack plot of the magnitude FT of FID signals detected for excitation pulses ranging from 3 to 6 ns. (b) Spectral coverage profile for a 3-ns excitation pulse recorded by overlapping the magnitude FT of FID signals detected at several magnetic fields. The dashed lines correct for the limited bandwidth of the quadrature mixer. The spectral coverage does not look symmetrical due to the frequency dependence of the conversion loss of the mixer employed in the receiver.

$\pi/2$ pulse should be about 5 ns, and the corresponding B_1 required is 17.9 G. Thus the resonator Q_L should be as small as 90 at 17 GHz to have the needed bandwidth, given that quadrature detection allows this to be obtained as ± 100 MHz. The shorter pulses lead to more uniform coverage in 2D ELDOR at the expense of a factor of 2–3 reduction in signal amplitude. With the DR, we have $\pi/2$ pulses of 3.6 ns at 2 kW for a small sample and 5 ns for a sample with length equal to that of the DR.

Reducing the losses in the waveguide elements at Ku band to 1.5–2 dB is possible, and it would help to obtain additional improvement in the spectral coverage. With a single 2.5-ns pulse, excitation of 150 G (420 MHz) is possible,

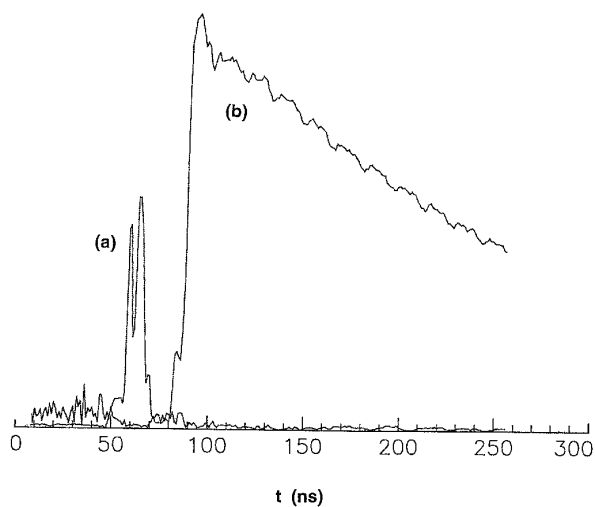


FIG. 3. Measurement of dead-time in a 2D ELDOR experiment. (a) The pulse reflected from the resonator is detected by the signal channel at high attenuation, and is seen as a narrow double peak on the left. (b) The magnitude of the FID signal from a small single crystal of TCNQ anion-radical salt, detected with the same signal channel, is plotted using the same time axis as (a). This measurement was made at 17.35 GHz, and it indicates a dead-time of about 30–35 ns for 2D ELDOR.

and 100 G (280 MHz) coverage may be achieved for 2D ELDOR with 3-ns pulses. The resonator volume also needs to be reduced 2–4 times to help obtain such coverage. Constructing a smaller BLGR working at Ku band is aided by the fact that the loop has a smaller inductance; hence a larger capacitance of the gaps is possible. With a reduction in volume by a factor of 4, such a resonator would allow us to routinely use 2.5-ns $\pi/2$ pulses. Rounded or bell-shaped pulses of width 2.5 ns are close to the shortest we can produce and deliver to the resonator.

At 17 GHz, a Q_L as small as 90 is adequate to obtain a resonator ring down time shorter than 30 ns. Figure 3 is an illustration of the dead-time measurement made at Ku band for 2D ELDOR with our spectrometer using the DR. Due to the sluggish falling edge of the gate of the TWTA that we use, a large noise signal is present for times shorter than 40 ns. This time can be reduced by about 5 ns by moving the mw pulse in the region where it starts to lose amplitude. At X band we also tested a TWTA with faster turn-off. This experiment was performed with an ASE117X TWTA, on loan from the Applied System Engineering (ASE) Corporation, which has a faster turn-off and lower output noise and provides a better quality pulse train than our 2 kW Logimetrics' EPA740I/J TWTA. We found that the output noise of the ASE's TWTA imposes only a 25-ns dead-time (Fig. 4). Its turn off time was 8 ns. It is seen in Fig. 4 that the averaged TWTA noise decays during the first 20 ns to the thermal noise background. [Added in proof: Through improvements on the Logimetrics TWTA, the dead-time has been shortened to 23–30 ns, at Ku band, depending on the

signal strength and the peak power used]. A high-power low-loss switch with a turn-off time of 1–5 ns, or an induction mode resonator with isolation of at least 40 db, would be an alternative way to deal with the TWTA noise, as we have previously noted (1).

The quality of 2D spectra at Ku band is as good as that at X band, because we are using quadrature phase shifters at their optimum frequency and conversion to Ku band does not introduce noticeable errors. Given the good phase accuracy, the 32-step ELDOR phase cycle (28) that we use works well at Ku band in eliminating all unwanted signals.

APPLICATIONS

Lipid Dispersions

To estimate the gain in sensitivity, we first selected a typical model lipid membrane sample, one for which good 2D ELDOR spectra at X band can readily be obtained. We used a sample of 0.5 mol% spin-labeled lipid, 16PC in DPPC (dipalmitoyl-L- α -phosphatidylcholine) hydrated with an excess of water. Samples with this concentration can readily be prepared, and it is typical for the CW-ESR experiments we have conducted. To illustrate the sensitivity improvement for small lipid samples at Ku-band, we reduced the amount of sample to just 1.5 μ L. The 2D ELDOR spectra in Fig. 5 were each acquired in 20 min. With a mixing time of 50 ns,

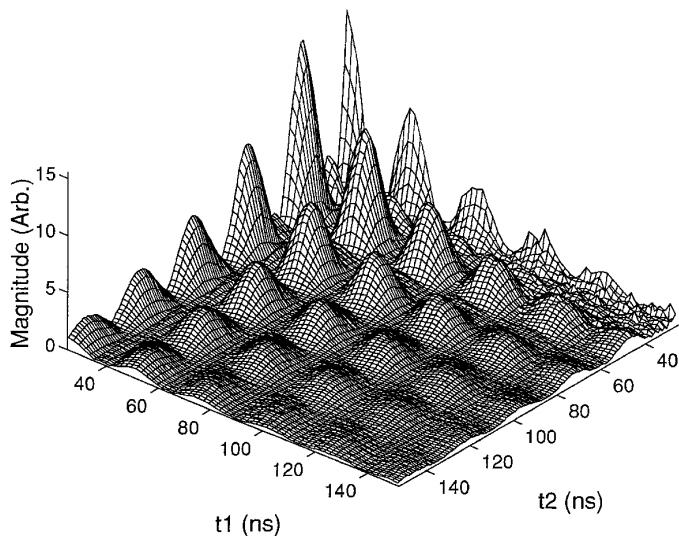


FIG. 4. Two-dimensional ELDOR data for 16PC in DMPG. The spectrum was collected at 9.2 GHz with an ASE117X TWTA. The magnitude stack plot of the S_c -2D ELDOR signal is plotted in the time domain as a function of t_1 and t_2 , where t_1 is the time interval between the first and second pulses and t_2 is the data acquisition time measured as the distance from the end of the third pulse. The pulse width was 5.6 ns for all 3 pulses. Data collection started from $t_1 = 25$ ns and $t_2 = 25$ ns. The mixing time was 400 ns. The rapidly decaying noise, observed during the first 20 ns of t_2 , is produced by the TWTA.

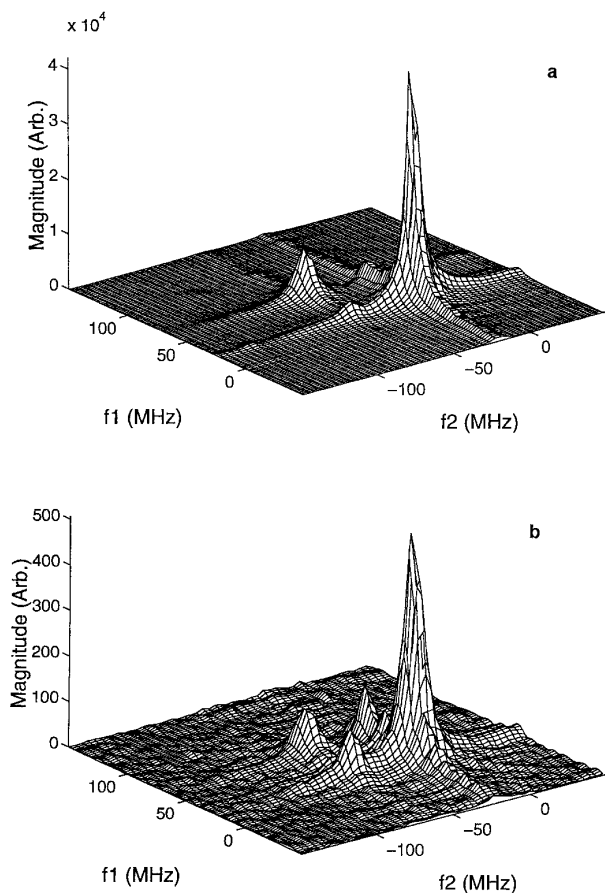


FIG. 5. Ku band 2D ELDOR magnitude spectra of 0.5 mol% 16PC in DPPC collected at 30°C. Sample volume was 1.5 μL and it was not deoxygenated. Mixing times were (a) $T_m = 50$ ns and (b) $T_m = 1$ μs . Spectra are plotted to a common scale.

the spectrum (Fig. 5a) exhibits a SNR of about 4000 for a total of 10 nmol of spin-probe. The high SNR may be very useful in looking for subtle effects in the 2D spectra. Alternatively, given that the SNR is about 10 times greater than what is usually required for detailed analyses, the number of spins in the sample can be safely decreased by a factor of 10–20 to 1–0.5 nmol. With a 3-h collection being a reasonable practical limit, an additional factor of 3 can be realized to reduce the above amounts to 0.33–0.17 nmoles, which would be adequate for natural spin-labeled biological samples. Finally, we note that practical data acquisition rates of ca. 50 kHz are now available, i.e., an increase by a factor of 5 over these experiments, which would enable a further reduction by a factor of $\sqrt{5}$.

Oriented Samples

As a second model system illustrating the performance at Ku band, a sample containing Cholestane (CSL) spin-probe was selected to give a signal that could not readily be ob-

tained at X band. Oriented phospholipid bilayers of egg yolk phosphatidylcholine (EYPC), containing 0.5–0.75 mol% of CSL spin-probe, were prepared following a procedure suggested by Shimoyama. Oriented lipid films were formed on $10 \times 1.8 \times 0.14$ mm glass substrates glued with epoxy to the flat end of a glass rod of 2 mm diameter. Initially, about 130 μL of chloroform stock solution, containing 1 mg of EYPC, was transferred to a vial and the chloroform was evaporated under nitrogen flow. Then 10 μL of 1 mM stock solution of CSL in chloroform was added, and the solution was carefully deposited on the substrate. After chloroform evaporation, the 100- μm films that were formed were then dried under nitrogen flow for 12 h followed by hydration at 35 C for 2 h by flowing 100% humidified nitrogen. In a glove bag under a nitrogen atmosphere, the substrate holder was placed into a standard 2.5-mm o.d. thin-walled glass sample tube. A small gap between the substrate edges and the tube walls was provided to prevent the film from creeping onto the tube wall. The assembly was then sealed with Hardman epoxy. CW EPR spectra confirmed that the films were well oriented. Two-dimensional ELDOR spectra were collected at 12 different mixing times, T_m ranging from 50 to

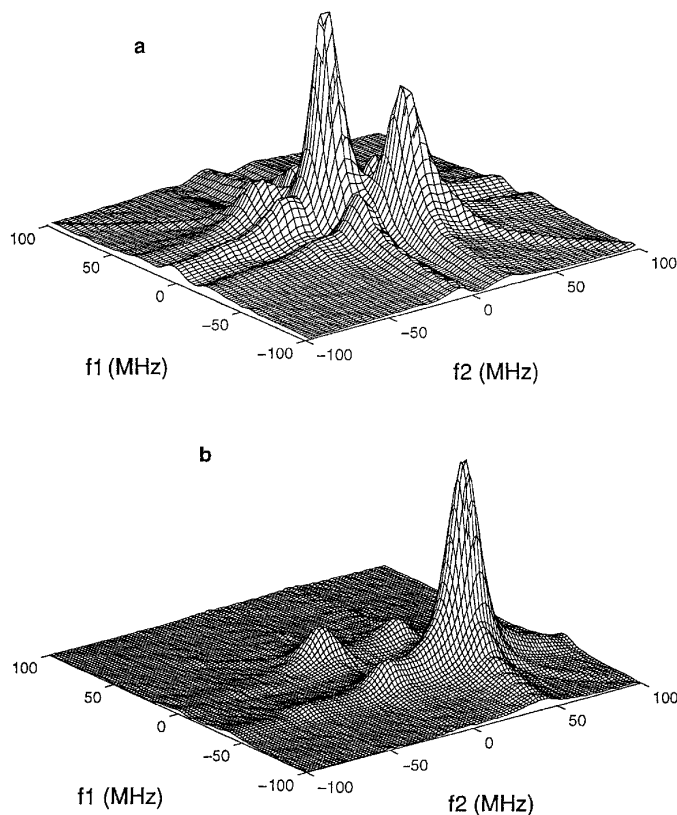


FIG. 6. Ku band 2D ELDOR magnitude spectra of 0.35 mol% CSL in macroscopically aligned membranes of EYPC at 30°C, obtained for two director tilt angles relative to the static magnetic field: (a) 0° and (b) 90°. Data were collected starting from $t_1 = 40$ ns, $t_2 = 40$ ns. Mixing time T_m was 50 ns in both spectra.

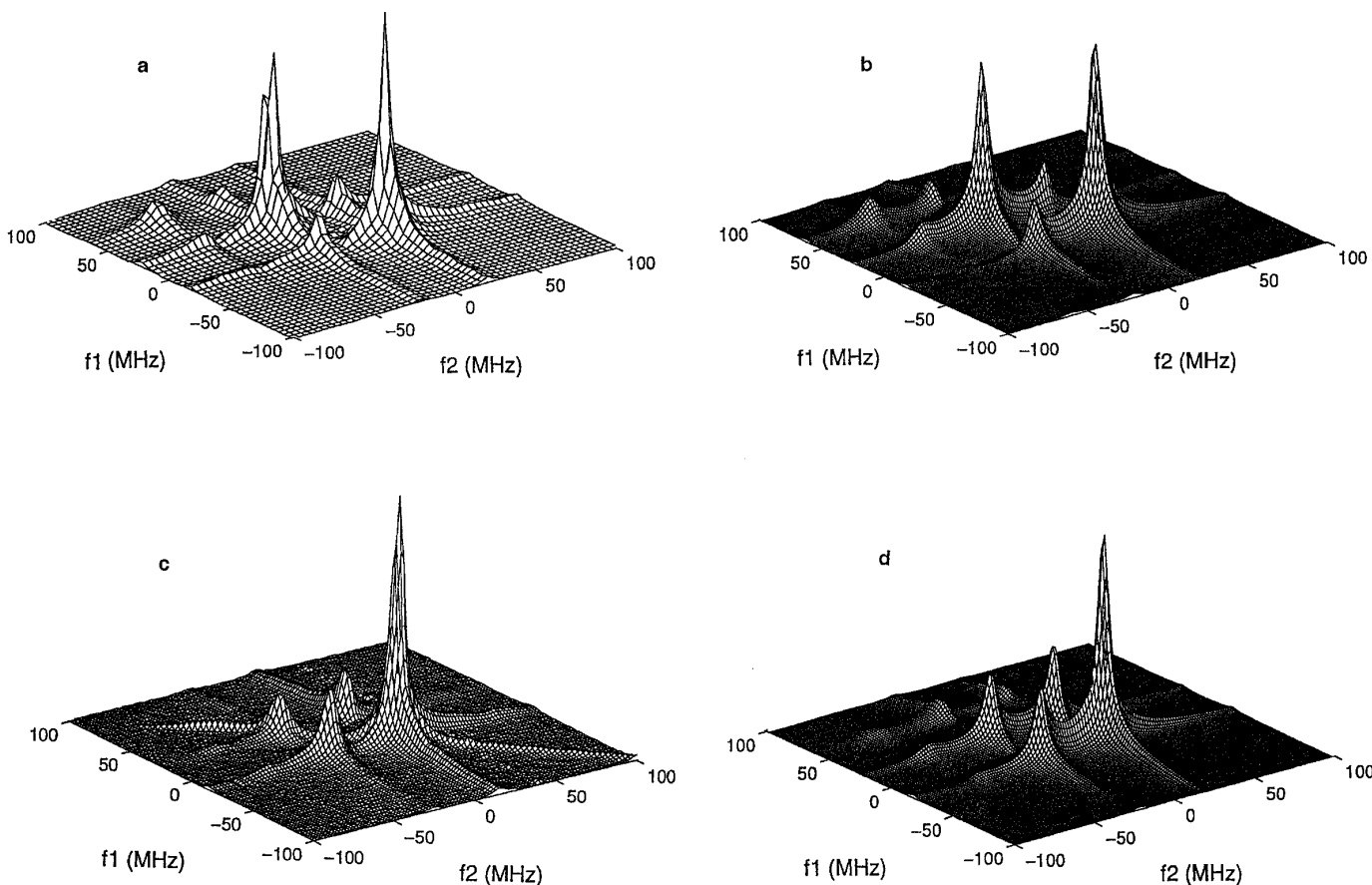


FIG. 7. Experimental and simulated 2D ELDOR spectra at frequencies of 9.3 and 17.35 GHz for the same sample of 16PC in DMPG at 36°C. (a) Magnitude 2D ELDOR spectrum collected at 9.3 GHz with $T_m = 100$ ns. (b) The fit to experimental spectrum (a) with the following model parameters: rotational diffusion rate $R = 9.8 \times 10^8 \text{ s}^{-1}$, $T_2 = 9.3 \times 10^{-8} \text{ s}$, orienting potential coefficient $C_0^2 = 0.23$, Heisenberg exchange rate, $\omega_{\text{HE}} = 0.69 \times 10^6 \text{ s}^{-1}$. (c) Magnitude 2D ELDOR spectrum collected at 17.35 GHz, with $T_m = 400$ ns. (d) Simulation of (c) using the model parameters given for (b).

2000 ns. Data collection at T_m of 50 ns was repeated two times in the course of the acquisition to monitor the decay of the CSL signal on the experimental time scale. For T_m shorter than 400 ns a collection time of 20 min gave a SNR better than 200 in the 2D ELDOR spectra. The whole experiment for two different sample orientations and all mixing times took 8 h. This performance was only possible with the improved sensitivity of the Ku band. The 2D ELDOR spectra of CSL in the oriented bilayers of EYPC are shown in Fig. 6 for director tilt angles with respect to the static magnetic field of 0° and 90°. The striking variation of the 2D ELDOR spectra at the two different orientations is clearly visible. We determined that the concentration of CSL in the sample at the start of the 2D ELDOR experiment was half that of a freshly prepared one, due to loss of CSL during preparation and storage periods; i.e., the sample contained only 5 nmol of spin-probe at the beginning of data collection.

Frequency Dependence

We also present 2D ELDOR spectra (cf. Fig. 7) obtained at both 9.3 and 17.35 GHz frequencies for the same sample

of 16PC in DMPG (1,2-dimyristoyl-*sn*-glycero-3-phosphoglycerol) hydrated with excess water. The Ku band 2D spectrum is markedly different from the X band spectrum, implying a slower motional regime, even though the motional rates have to be the same at both frequencies. The experimental 2D ELDOR X band spectrum (Fig. 7a) was fitted with the NLLS software package (38) using a Brownian rotational diffusion model. Then with the optimized set of fitting parameters we simulated the 2D ELDOR spectrum at Ku band. As is seen from Figs. 7c and 7d, the simulated spectrum is in good agreement with experiment.

FURTHER IMPROVEMENTS

To obtain greater sensitivity for samples of limited size, it would be desirable to use higher frequencies, such as 35 GHz. Other possibilities for improvement are the same for all frequencies. The pulse repetition of 10 kHz that we used may be increased 5 to 10 times to 50–100 kHz as noted above. At full power this is possible with microwave pulses as short as 5 ns, because the average microwave power

dissipated in a lossy sample will be tolerable. A faster signal digitizer operating at a rate of 500–1000 Msps would give us another factor of 2.5–5 in rate of data acquisition. All combined, these improvements would result in a factor of 5 improvement in the SNR for the same 3-h experiment. Therefore, the minimum number of spins sufficient for obtaining 2D spectra suitable for reliable analysis (i.e., SNR of 200–400) would be 70–30 pmol for the case of 16PC and 700–300 pmol for CSL. With a dead-time of 20–25 ns, which we hope to achieve, the situation would be improved for CSL by an additional factor of 2–3. Speaking in terms of the minimum *detectable* number of spins (SNR = 1) in a 2D experiment we estimate it would be 16PC at Ku band per 3 hours or 1.2×10^{13} spins/s^{1/2} if the spectrum is to be detected in 1 s. Currently it is 6×10^{13} spins/s^{1/2}. An estimate of the minimum detectable number of spins per unit time made with Eq. [5] and using parameters close to those appropriate for 16PC yielded the value of 2×10^{13} spins/s^{1/2}, which is close to the experimentally determined sensitivity. One word of caution in these estimates is that they have been based upon an analysis using moderate to strong signals. Very weak signals, that are affected by the low-noise “tail” of the TWTA output, suffer more degradation in SNR.

CONCLUSIONS

1. We have shown that 2D FT ESR spectroscopy benefits from extension to higher frequencies. We showed, using the model system of 16PC in DMPG, that the 2D ELDOR spectrum of this spin-probe exhibits a large change with frequency. Fitting 2D ELDOR spectra, obtained at different frequencies, with the same set of ordering and dynamic parameters would help to refine the model of molecular dynamics.

2. At Ku band, the sensitivity has been considerably improved. The concentration sensitivity at Ku band is 4–8 times better than we were able to achieve at X band. This is of particular value for studies of biological samples that are not available in large amounts or of samples that are very dilute. Combined with shorter dead-times, it allows us to experiment with less than 1 nmol of spins, with T_2 values as short as 30 ns. Most important, we were able to extend 2D ELDOR experiments to microscopically aligned lipid membranes with a total amount of material as small as 1 mg. For a system with $T_2 \geq 50$ ns, 100 pmol of spin-probe is sufficient for a full 3D ELDOR data collection (i.e., with T_m stepped out for the 3rd dimension).

3. We have shown that the dead-time of our spectrometer is improved at Ku band and is typically 30–40 ns, with shorter times possible.

4. We demonstrated that an extension of the frequency range of an ESE spectrometer using a heterodyne scheme can be made with minimal investments provided a suitable

excitation source is available. Another feature important for a heterodyne 2D FT ESR spectrometer is that its frequency can be tuned without losing the accuracy of the phase shifting, because it is determined at the fixed frequency where the precision of the phase shifter can be made very high.

5. The spectrometer that we built also has great potential for FID or 1D FT spectroscopy applied to studies of transient chemical intermediates. We are able to apply pulses as narrow as 2.5 ns and to achieve spectral coverage well in excess of 100 G. The dead-time is routinely in the range of 35–40 ns with a proper subtraction scheme. Operation at more than one frequency is an additional benefit, providing extra information useful in the interpretation of the time-resolved experiment.

ACKNOWLEDGMENTS

The authors are grateful to Applied Systems Engineering, Inc., for the opportunity to test their TWTA with our spectrometer. We also express thanks for the assistance of Dianne Patzer and for helpful discussions with Curt Dunnam. Dr. Mingtao Ge's help with preparation of the 16PC sample is greatly appreciated. This work was supported by Grants GM25862 and RR07126 from the National Institutes of Health and Grant CHE9301027 from the National Science Foundation.

REFERENCES

1. J. Gorcester, G. H. Millhauser, and J. H. Freed, in “Modern Pulsed and Continuous Wave Electron Spin Resonance” (L. Kevan and M. K. Bowman, Eds.), pp. 119–194, Wiley, New York (1990).
2. M. K. Bowman, in “Modern Pulsed and Continuous Wave Electron Spin Resonance” (L. Kevan and M. K. Bowman, Eds.), pp. 2–42, Wiley, New York (1990).
3. J. Gorcester, S. B. Ranavarave, and J. H. Freed, *J. Chem. Phys.* **90**, 5764–5786 (1989).
4. V. S. S. Sastry, A. Polimeno, R. H. Crepeau, and J. H. Freed, *J. Chem. Phys.* **105**(14), 5753–5772 (1996); *J. Chem. Phys.* **105**, 5773 (1996).
5. D. Xu, R. H. Crepeau, C. K. Ober, and J. H. Freed, *J. Phys. Chem.* **100**, 15,873–15,895 (1996).
6. R. H. Crepeau, S. Saxena, S. Y. Lee, B. R. Patyal, and J. H. Freed, *Biophys. J.* **66**, 1489–1504 (1994).
7. B. R. Patyal, R. H. Crepeau, and J. H. Freed, *Biophys. J.*, in press.
8. D. E. Budil, K. A. Earle, and J. H. Freed, *J. Phys. Chem.* **97**, 1294–1303 (1993).
9. J. Gorcester and J. H. Freed, *J. Chem. Phys.* **88**(8), 4678–4693 (1988).
10. R. R. Ernst, G. Bodenhausen, and A. Wokaun, “Principles of Nuclear Magnetic Resonance in One and Two Dimensions,” Clarendon, Oxford (1987).
11. A. Angerhofer, R. J. Massoth, and M. K. Bowman, *Israel J. Chem.* **28**, 227–238 (1988).
12. M. Pluschau, G. Kroll, K.-P. Dinse, and D. Beckert, *J. Phys. Chem.* **96**, 8820 (1992).
13. C. J. Kleverlaan, D. M. Martino, H. van Willigen, D. J. Stufkens, and Ad Oskam, *J. Phys. Chem.* **100**, 18,607–18,611 (1996).
14. G. L. Millhauser and J. H. Freed, *J. Chem. Phys.* **81**, 37 (1984).

15. L. J. Schwartz, G. L. Millhauser, and J. H. Freed, *Chem. Phys. Lett.* **127**, 60–66 (1986).
16. J. Gorcester and J. H. Freed, *J. Chem. Phys.* **85**, 5375 (1986).
17. B. R. Patyal, R. H. Crepeau, D. Gamliel, and J. H. Freed, *Chem. Phys. Lett.* **175**, 445–452 (1990); *Chem. Phys. Lett.* **175**, 453–460 (1990).
18. S. Y. Lee, B. R. Patyal, and J. H. Freed, *J. Chem. Phys.* **98**, 3665–3689 (1993).
19. W. B. Mims in "Electron Paramagnetic Resonance" (S. Geschwind, Ed.), p. 234, Plenum, New York (1972).
20. A. Schweiger, in "Modern Pulsed and Continuous-Wave Electron Spin-Echo Resonance" (L. Kevan and M. K. Bowman, Eds.), p. 112, Wiley, New York (1990).
21. J. J. Shane, "Electron Spin Echo Envelope Modulation Spectroscopy of Disordered Solids," Ph.D. thesis, p. 3 Nijmegen (1993).
22. J. Allgeier, J. A. J. M. Disselhorst, R. T. Weber, W. Th. Wenckebach, and J. Schmidt, in "Modern Pulsed and Continuous-Wave Electron Spin Resonance" (L. Kevan and M. K. Bowman, Eds.), pp. 267–282, Wiley, New York (1990).
23. T. F. Prisner, "Pulsed High-Field/High-Frequency EPR," Habilitation Thesis, Department of Physics, Free University of Berlin (1995).
24. J. Hornak and J. H. Freed, *J. Magn. Reson.* **67**, 501–518 (1986).
25. K. M. Salikhov, A. G. Semenov, and Yu. D. Tsvetkov, "Electron Spin-Echo and Its Applications," Novosibirsk, Nauka (1976).
26. C. E. Davoust, P. E. Doan, and B. M. Hoffman, *J. Magn. Reson. A* **119**, 38–44 (1996).
27. T. F. Prisner, S. Un, and R. G. Griffin, *Isr. J. Chem.* **32**, 357–363 (1992).
28. D. Gamliel and J. H. Freed, *J. Magn. Reson.* **89**, 60–93 (1990).
29. M. Suki, G. A. Rinard, S. S. Eaton, and G. R. Eaton, *J. Magn. Reson. A* **118**, 173–188 (1996).
30. W. Piasecki, W. Froncisz, and J. S. Hyde, *Rev. Sci. Instrum.* **67**(5), 1896–1904 (1996).
31. B. E. Sturgeon and R. D. Britt, *Rev. Sci. Instrum.* **63**, 2187–2192 (1992).
32. P. Borbat and A. Raitsimring, New pulsed electron spin-echo spectrometer of University of Arizona, in "Abstracts of 36th Rocky Mountain Conference on Analytical Chemistry, Denver, 1994," p. 94.
33. S. Saxena and J. H. Freed, *Chem. Phys. Lett.* **251**, 102 (1996).
34. K. Holczer, D. Schmalbein, and P. Barker, *BRUKER Rep.* **2**, 4 (1988).
35. K. M. Salikhov, D. J. Schneider, S. Saxena, and J. H. Freed, *Chem. Phys. Lett.* **262**, 17–26 (1996).
36. P. Borbat and A. Raitsimring, *J. Magn. Reson. A* **114**, 261–263 (1995).
37. G. R. Rinard, R. W. Quine, S. S. Eaton, G. R. Eaton, and W. Froncisz, *J. Magn. Reson. A* **108**, 71–81 (1994).
38. D. E. Budil, S. Y. Lee, S. Saxena, and J. H. Freed, *J. Magn. Reson. A* **120**, 155–189 (1996).